

Biosynthetic Pathway for High Structural Diversity of a Common Dilactone Core in Antimycin Production

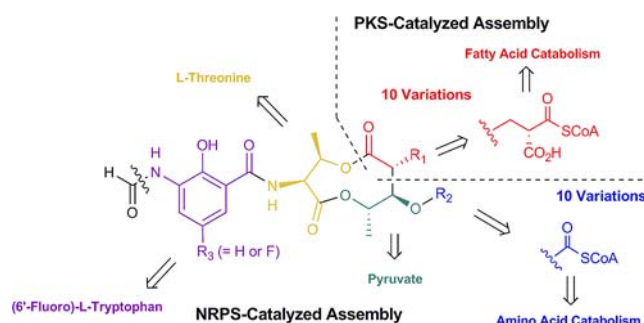
Yan Yan,[†] Lihan Zhang,[‡] Takuya Ito,[§] Xudong Qu,^{*,†} Yoshinori Asakawa,[§]
Takayoshi Awakawa,[‡] Ikuro Abe,[‡] and Wen Liu^{*,†}

State Key Laboratory of Bioorganic and Natural Products Chemistry,
Shanghai Institute of Organic Chemistry, Chinese Academy of Sciences, 345 Lingling
Road, Shanghai 200032, China, Graduate School of Pharmaceutical Science, University
of Tokyo, 7-3-1 Hongo, Bunkyo-ku 113-0033, Japan, and Faculty of Pharmaceutical
Sciences, Tokushima Bunri University, Yamashiro-cho, Tokushima 770-8514, Japan

xudongqu@gmail.com; wliu@mail.sioc.ac.cn

Received June 29, 2012

ABSTRACT



We herein report comparative analysis of two versions of the biosynthetic gene clusters of antimycins, a natural product family possessing up to 44 distinct entities. The biosynthetic pathway of antimycins is amenable to the high structural variation of the substrates, supported by successes in heterologous expression of the *ant* cluster and in fluorine incorporation. The latter facilitated the investigation of the structure–activity relationship into the usually invariable 3-formamidosalicylic acid moiety of the molecules.

Antimycin (ANT) antibiotics, with a remarkable variety of biological activities, constitute a natural product family now comprising up to 44 distinct entities.¹ They share a nine-membered dilactone core conjugated with an unusual 3-formamidosalicylic acid (FSA) moiety (Figure 1). The major differences of the members are present at the C7 and C8 positions of the core system, with the substitutions of

carbon side chains highly varying in length and branching (Figure S1). Important advances regarding ANT biosynthesis were developed recently. In 2011, Hutchings and co-workers first mined an *ant* cluster from the genome of an attine ant-symbiotic strain *Streptomyces* sp. S4.^{2a} In 2012, Spiteller and co-workers characterized anthranilate as a key intermediate during the conversion of L-tryptophan into FSA.^{2b} However, the ANT biosynthetic pathway remains to be established. In this study, we focus on the analysis of the genetic basis for ANT production, aimed at providing an overall understanding in the biosynthesis to account for the high structural variation of individual members.

[†] Chinese Academy of Sciences.

[‡] University of Tokyo.

[§] Tokushima Bunri University.

(1) (a) Leben, C. *Phytopathology* **1949**, *39*, 13. (b) Yang, Y.-Q.; Wu, Y. *Org. Prep. Proced. Int.* **2007**, *39*, 135–152. (c) Walsh, C. T.; Haynes, S. W.; Ames, B. D. *Nat. Prod. Rep.* **2012**, *29*, 37–59. (e) Slater, E. C. *Biochim. Biophys. Acta* **1973**, *301*, 129–154. (f) Tzung, S. P.; Kim, K. M.; Basanez, G.; Giedt, C. D.; Simon, J.; Zimmerberg, J.; Zhang, K. Y. J.; Hockenbery, D. M. *Nat. Cell Biol.* **2001**, *3*, 183–191. (g) Kido, G. S.; Sphalski, E. *Science* **1950**, *112*, 172–173. (h) Birch, A. J.; Harada, Y.; Cameron, D. W.; Rickards, R. W. *J. Chem. Soc.* **1961**, 889–895. (i) Neft, N.; Farley, T. M. *J. Antibiot. (Tokyo)* **1972**, *25*, 298–303.

(2) (a) Seipke, R. F.; Barke, J.; Brearley, C.; Hill, L.; Yu, D. W.; Goss, R. J. M.; Hutchings, M. I. *PLoS One* **2011**, *6*, e22028. (b) Schoenian, I.; Paetz, C.; Dickschat, J. S.; Aigle, B.; Leblond, P.; Spiteller, D. *ChemBioChem* **2012**, *13*, 769–773.

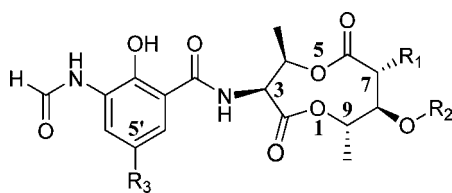


Figure 1. Core structure of ANTs. For details of naturally occurring members ($R_3 = H$), please see Figure S1. Fluorinated analogues in this study. 5'-F-A_{2a}: $R_1 = CH_2(CH_2)_4CH_3$, $R_2 = CO(CH_3)_2$, and $R_3 = F$; 5'-F-A_{4a}: $R_1 = CH_2(CH_2)_2CH_3$, $R_2 = CO(CH_3)_2$, and $R_3 = F$.

Given the fact that a number of *Streptomyces* strains are known to produce ANTs, we employed a genome comparison strategy to access the genetic basis. Two different producing strains, *Streptomyces* sp. NRRL 2288 and *S. blastmyceticus* NBRC 12747, were subjected to sequencing, yielding the genome drafts for comparative analysis. This allowed identification of a genetic locus highly conserved in sequence (51–68% identities) and organization from both strains, containing 15 or 17 genes that include a cassette (*antC-D*) encoding a nonribosomal peptide synthetase (NRPS)/polyketide synthase (PKS) hybrid system (Figure 2A). Compared to the 15-gene cluster from the NRRL 2288 strain (namely *ant₁*, with a sequence accession number JX131329), the relatively longer 17-gene cluster from the NBRC 12747 strain (namely *ant₂*, JX137118) has two additional genes encoding a pathway-specific kynureninase (*ant₂P*) and a phosphopantetheinyl transferase (PPTase) (*ant₂Q*), respectively (Tables S3A and S3B). To correlate the identified locus with ANT production, we chose the NRPS gene *ant₁C* for inactivation (Figure 3, VII). The resulting mutant strain failed to produce ANTs, supporting the fact that ANTs are a group of nonribosomal peptide–polyketide hybrid molecules in biosynthesis.

Hutchings and co-workers have identified two *ant*-like gene clusters respectively from two genome-sequenced strains (Figure 2A), *S. albus* J1074^{3a} (for *ant₃*) and *S. ambofaciens* ATCC 23877^{3b} (for *ant₄*), by using the cluster (namely *ant₅*) from *Streptomyces* sp. S4 as the reference.^{2a} Taking all the available into account, we found that these five clusters falls into two forms different in length, dependent on the absence or presence of two additional genes *antP* and *antQ*. While the three 15-gene clusters, *ant₁*, *ant₃*, and *ant₅*, are nearly identical (97–100% identities) in a short (S)-form, the two 17-gene clusters, in a long (L)-form, share the head-to-tail homology (38–81% identities) to each other but differ in the flanking region. To confirm the ANT-producing potential of the strains J1074 and ATCC 23877, we fermented them and subsequently examined the product profiles. Indeed, UV absorbance-coupled HPLC-MS analysis revealed that they both produced a number of ANTs (Figure 3, III and IV). The PKS genes *ant₃D* and *ant₄D* in these strains were accordingly

inactivated, leading to complete abolition of ANT production (Figure 3, VIII and IX). These findings provided the experimental evidence to support the uniform paradigm for ANT biosynthesis in J1074, S4, and ATCC 23877 as well as NRRL 2288 and NBRC 12747.

We thus proposed that ANT biosynthesis in various producing strains employs a common NRPS/PKS system to assemble the skeleton (Figure 2B). The process may begin with the utilization of FSA as a starter unit, the formation of which can share certain steps with tryptophan degradation in cells.^{1h,i} AntN, a putative tryptophan 2,3-dioxygenase, could catalyze an oxidative C–C bond cleavage to give *N*-formyl kynurenine. This compound, after a deformylation, is subsequently converted into anthranilate by AntP, a putative kynureninase. AntHIJKL are homologous to the proteins PaaABCDE in the phenylacetyl-CoA catabolic pathway.⁴ They may act on the 2-aminobenzoate moiety, which is assumed to be activated by CoA ligase-like protein AntF in a peptidyl carrier protein (PCP) AntG-tethered form, to participate in an epoxidation-coupled rearrangement to afford FSA (Figure 2B). This reconstitution, recently confirmed by Spitteller and co-workers,^{2b} involves a 1,2-shift of a carboxylate. AntC, a two module (M) NRPS containing a N-terminal condensation (C), adenylation (A), PCP, central C, A, ketoreductase (KR), and C-terminal PCP domains, is presumably able to catalyze the sequential elongation by using L-threonine (Figure S4A) and pyruvate as the extender units. AntC-M2, similar to Cesa and CesB for α -keto acid activation and subsequent keto-reduction by the internal KR domain,⁵ is likely responsible for building the first ester bond of the dilactone core. AntD, a PKS composed of the ketosynthase (KS), acyltransferase (AT), acyl carrier protein (ACP), and thioesterase (TE) domains, could then take over the linear intermediate and catalyze a two-carbon extension to furnish the second ester bond by subsequent cyclization/lactonization (Figure 2B).

Based on the above NRPS/PKS assembly logic, we reasoned that the diversity may first take place in the PKS AntD-catalyzed elongation. Analysis of the specificity-conferring motifs revealed that AntD-AT is distinct from those normally for malonyl-CoA, methylmalonyl-CoA, or ethylmalonyl-CoA (Figure S3B), indicating the potential with a broadened cavity for substrate binding. For the AT substrate supply, we identified a crotonyl-CoA reductase/carboxylase (CCR)-encoding gene *antE* in the *ant* clusters (Figure 2A). CCRs have recently been recognized for their substrate tolerance, as different alkylmalonyl-CoAs can be synthesized via a reductive carboxylation of their *E*-2,3-ene precursors (originating from fatty acid metabolism, Figure 2B).⁶ However, AntE and its functionally associated AntD-AT are predicted to be extremely promiscuous in extender unit generation and

(4) Teufel, R.; Mascaraque, V.; Ismail, W.; Voss, M.; Perera, J.; Eisenreich, W.; Haehnel, W.; Fuchs, G. *Proc. Natl. Acad. U.S.A.* **2010**, *107*, 14390–14395.

(5) (a) Marahiel, M. A.; Stachelhaus, T.; Mootz, H. D. *Chem. Rev.* **1997**, *97*, 2651. (b) Magarvey, N. A.; Ehling-Schulz, M.; Walsh, C. T. *J. Am. Chem. Soc.* **2006**, *128*, 10698–10699.

(6) Quade, N.; Huo, L.; Rachid, S.; Heinz, D. W.; Mueller, R. *Nat. Chem. Biol.* **2012**, *8*, 117–124.

(3) (a) Rubinstein, E.; Keller, N. *J. Antimicrob. Chemother.* **1998**, *42*, 572–576. (b) Baltz, R. *J. Ind. Microbiol.* **2010**, *37*, 759–772.

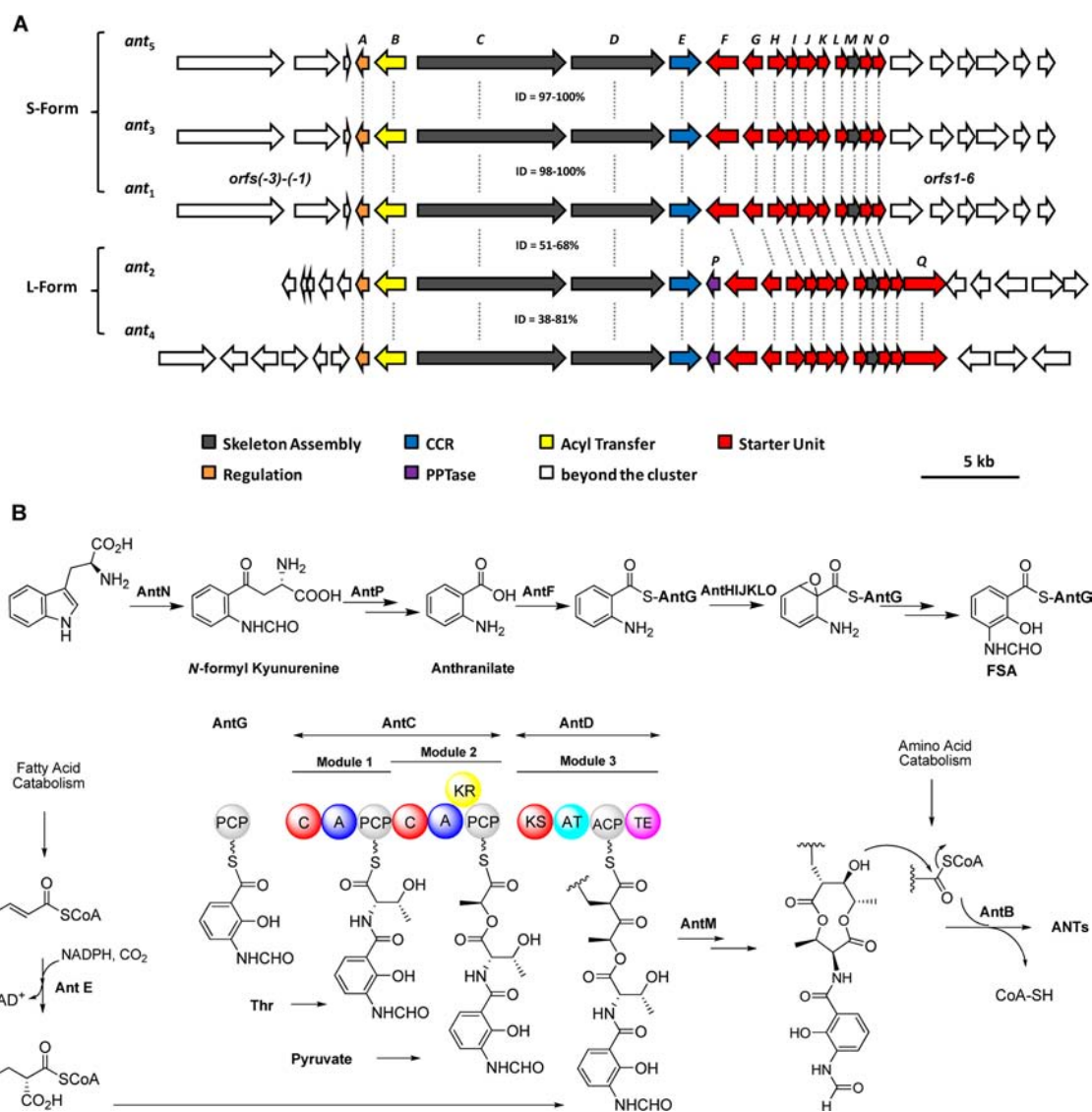


Figure 2. Biosynthetic gene clusters and proposed pathway. (A) Gene organization of the *ant* clusters from various producing *Streptomyces* strains, including NRRL 2288 (for *ant*₁), NBRC 12747 (for *ant*₂), J1074 (for *ant*₃), ATCC 23877 (for *ant*₄), and S4 (for *ant*₅). For *ant*₁ and *ant*₂, the deduced functions of the genes are labeled in color and summarized in Tables S3A and S3B. ID, sequence identity. (B) Hypothesis for the FSA moiety formation, NRPS/PKS-catalyzed skeleton assembly, and postmodification in ANT biosynthesis. The functional domains are indicated in color.

recognition to build the C7 side carbon chain, given the presence of its 10 structural variations (in a length-variable linear or branching form, or in an aromatic form, Figure S1) in the ANT family. The diversity can then occur in the NRPS/PKS-post tailoring stage. This requires a C8 ketoreduction, presumably catalyzed by an oxidoreductase AntM, to afford the hydroxyl group for acyl appending. AntB, a putative acyltransferase, likely catalyzes the transfer of different acyl groups, some of which may derive from the metabolism of amino acids, to construct the C8 side chain that currently has 10 variations in total (Figures 2B and S1).

The S-form gene cluster *ant*₁ was then chosen for heterologous expression. We first constructed a genomic library of NRRL 2288 and identified a 44 kb DNA fragment-containing fosmid by using the CCR gene *ant*_{1E}

as a probe. Sequencing analysis revealed that the entire *ant*₁ flanks a truncated upstream *nrrps* [*orf*(-2)] and downstream genes (*orf*1-9) nearly identical to those found in *Streptomyces* sp. FR-008 for candicidin biosynthesis.⁷ This fosmid was then subjected to engineering (Figure S2), to integrate the elements for conjugal introduction (*ori*T) and site-specific recombination onto the chromosome (ϕ C-31 site and its associated integrase gene). Next, the engineered fosmid was introduced into two genome sequence-available hosts *S. lividans* and *S. coelicolor*, respectively, which apparently lack the genetic basis to produce ANTs. In contrast to no change of growth manner

(7) Chen, S.; Huang, X.; Zhou, X. F.; Bai, L. Q.; He, J.; Jeong, K. J.; Lee, S. Y.; Deng, Z. X. *Chem. Biol.* **2003**, *10*, 1065-1076.

and morphology found in the *S. coelicolor* recombinant strain during a 7-day cultivation, cells of the *S. lividans* recombinant strain were suddenly lysed on day 3. Finally, HPLC-MS analysis of the culture extract of the *S. coelicolor* strain was performed, indeed showing that this strain produced a set of ANTs (Figure 3, VI). These findings clearly indicated that the *ant* cluster, even in an S-form, contains all the genetic elements for generating the FSA-conjugated dilactone core and particularly its structural diversity.

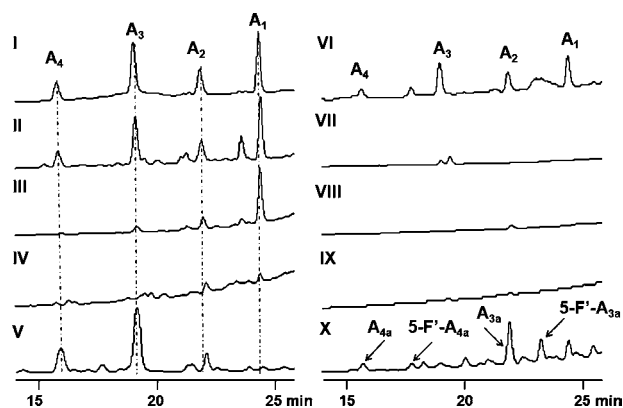


Figure 3. HPLC analysis of ANT production. I, standard; II, *S. sp.* NRRL 2288; III, *S. albus* J1074; IV, *S. ambofaciens* ATCC 23877; V, *S. blastomyces* NRBC 12747; VI, AL2612 (*S. coelicolor* M145 carrying the *ant*₁ cluster); VII, AL2101 (*S. sp.* NRRL 2288 derivative, Δant_1C); VIII, AL2301 (*S. albus* J1074 derivative, Δant_3D); IX, AL2401 (*S. ambofaciens* ATCC 23877 derivative, Δant_4D); and X, *S. sp.* NRRL 2288 supplemented with 6-fluoro-L-tryptophan. For the standard (A₁-A₄, Figure 1 as the reference), the components “a” and “b” have not been chemically discriminated. A₁: R₁ = CH₂(CH₂)₄CH₃, R₂ = COCH(CH₃)CH₂CH₃ (A_{1a}) or COCH₂CH(CH₃)₂ (A_{1b}); A₂: R₁ = CH₂(CH₂)₄CH₃, R₂ = COCH(CH₃)₂ (A_{2a}) or COCH₂CH₂CH₃ (A_{2b}); A₃: R₁ = CH₂(CH₂)₂CH₃, R₂ = COCH(CH₃)CH₂CH₃ (A_{3a}) or COCH₂CH(CH₃)₂ (A_{3b}); and A₄: R₁ = CH₂(CH₂)₂CH₃, R₂ = COCH(CH₃)₂ (A_{4a}) or COCH₂CH₂CH₃ (A_{4b}).

Spiteller and co-workers showed that the FSA moiety of ANTs can tolerate the structural alteration in biosynthesis, such as fluorination;^{2b} however, the resulting FSA-fluorinated analogues have not been characterized individually. To evaluate the effect of fluorine incorporation on the biological activity, we fed 6-fluoro-L-tryptophan, other than previously used fluoroanthranilate intermediates,^{2b} into the producing NRRL 2288 strain for fermentation. HPLC-MS analysis of the culture broth showed that, indeed, a set of fluorinated ANTs were produced with

their associated natural entities (Figure 3, X). Four compounds were purified and subsequently characterized to be the pairs A_{2a}/5'-F-A_{2a} and A_{4a}/5'-F-A_{4a} on the basis of HR-ESI-MS and NMR analyses (Supporting Information). New compounds 5'-F-A_{2a} and 5'-F-A_{4a} (Figure S9) were then subjected to bioassays, with their parent compounds A_{2a} and A_{4a}, and the standard component A_{3b}, as the controls. For the test using the mouse leukemia P388 cell line, the activity of 5'-F-A_{2a} or 5'-F-A_{4a} dramatically decreased, with a 50% inhibiting concentration (IC₅₀, at 0.35 μ g/mL for 5'-F-A_{2a} or at 3.5 μ g/mL for 5'-F-A_{4a}) 6-fold lower than that of A_{2a} or A_{4a} (Table S5B). This is likely due to the change in the binding manner of ANTs to target proteins, as 5'-fluorination can alter the charge distribution of the benzene ring of FSA. In contrast, the fluorinated compounds retained the potent antifungal activity against the test strain *Candida albicans*, which was comparable (if not, only slightly decreased) to that of the corresponding parent compounds (Figure S10). These results suggest that the less cytotoxic, ANT-like fungicides, which are potentially more safe to mammals, can be developed by FSA modification.

In conclusion, we uncovered a uniform paradigm for ANT biosynthesis, by characterization of the *ant* clusters (in S-form or L-form) from various producing *Streptomyces* strains. They employ a hybrid NRPS/PKS system to program the skeleton assembly of the FSA-conjugated dilactone core. The results strongly supported an overall compatibility of the ANT biosynthetic machinery that remarkably tolerates the change of the very early substrate to generate the fluorinated starter unit 5-F-FSA and then to initiate the extender unit-variable assembly process followed by postmodification of the different acyl groups. The findings reported here now pave the way for ongoing biochemical investigations into mechanisms for this diversity.

Acknowledgment. We thank Dr. Cesar Sanchez, Universidad de Oviedo, for providing *S. albus* J1047. This work was supported in part by grants from the NNSF (30900021, 20832009, and 20921091), “973 program” (2010CB833200 and 2012CB721100), CAS (KJCX2-YW-201) of China, and Grants-in-Aid for Scientific Research from the Ministry of Education, Culture, Sports, Science and Technology, Japan.

Supporting Information Available. Experimental details. This material is available free of charge via the Internet at <http://pubs.acs.org>.

The authors declare no competing financial interest.